Fault-Tolerant Control for Non-sinusoidal Seven-phase PMSMs with Similar Copper Losses

Duc Tan Vu, Ngac Ky Nguyen, Eric Semail, Trung Hai Do

Fault-Tolerant Control for Non-sinusoidal Seven-phase PMSMs with Similar Copper Losses

Duc Tan Vu[1,2], Ngac Ky Nguyen[1], Eric Semail[1], Trung Hai Do[2]

[1]*Univ. Lille, Arts et Metiers Institute of Technology, Central Lille, Junia, ULR 2697 - L2EP, F-59000 Lille, France*

[2]*Thai Nguyen University of Technology, Thai Nguyen University, Thai Nguyen 250000, Vietnam*

vuductan-tdh@tnut.edu.vn; ngacky.nguyen@ensam.eu; semail.eric@ensam.eu; dotrunghai@tnut.edu.vn

***Abstract*—This paper proposes a strategy using new transformation matrices to calculate new current references when a non-sinusoidal seven-phase permanent magnet synchronous machine (PMSM) has an open-circuited phase. The new current references allow to obtain a smooth torque with similar copper losses in the remaining healthy phases even when the back electromotive force (back-EMF) is non-sinusoidal. A real-time current learning process using an adaptive linear neural network (Adaline) is applied to extract from measured currents useful harmonic components in torque generation. It improves torque quality, especially at high speed, even when standard proportional-integral (PI) controllers are applied. In addition, similar copper losses in the remaining phases with the new current references can avoid overheating of windings. The effectiveness of the proposed control strategy is validated by numerical results.**

***Keywords*—Multiphase machine, seven-phase PMSM, non-sinusoidal back-EMF, fault-tolerant control, Adaline, similar copper loss.**

I. INTRODUCTION

ELECTRIC drive systems with variable speeds using multiphase machines have been more attractive since the last decades owing to technology evolution of semiconductors and microprocessors. The ability to tolerate faults of electric machine drives and the reduction in per phase converter power rating make multiphase machines dominant compared to three-phase machines [1]. In electric drives, open-circuit or short-circuit faults may happen in stator windings or power converters. Among them, open-circuit types are the most frequent faults [2]. In post-fault operations, a reconfiguration of current control is required so that the drives can operate without torque pulsations, overrated currents and voltages. Owing to more degrees of freedom than three-phase machines, the fault-tolerant operations of multiphase machines can be undertaken without any additional hardware. The common idea of post-fault current reconfigurations is to maintain the magnetomotive forces (MMFs) like in healthy mode as early presented in [3, 4] for induction machines and recently described in [5] for synchronous machines.

Indeed, to preserve the healthy MMFs, the approach in [6, 7] was proposed to obtain constant currents in d-q reference frames that are associated with main harmonics, creating most of the torque. This approach does not require any modification of the Clarke transformation matrix and PI controllers. However, in other frames, d-q currents are time-variant. If the corresponding harmonics of back-EMF exist, the torque ripple becomes significant. Studies [6, 7] can reduce the torque ripple with more constant current references for PI controllers. However, new phase currents generate different copper losses in the remaining healthy phases, possibly leading to overheating of a phase winding.

Similarly, based on [3, 4], many studies using reduced-order transformation matrices under open-circuit faults have been introduced in recent years. New transformation matrices with orthogonality property are derived from post-fault mathematical models of the drives. However, most of these studies [8-12] only deal with sinusoidal back-EMFs. If these methods are applied to non-sinusoidal machines, high torque ripples are dramatically generated because of interactions between back-EMF harmonics and the fundamental current as analyzed in [13]. Only studies [14-16] consider non-sinusoidal machines with the presence of the 3rd harmonic of back-EMF. Study [14] applies two new Clarke matrices for the 1st and 3rd harmonics to obtain phase current references. Torque ripples due to the 3rd harmonic of back-EMF are eliminated by the injection of the 3rd harmonic current. However, all new current references in rotating frames for control are not constant, leading to a reduction in torque quality with PI controllers at high speed. Meanwhile, strategies in [15, 16] are proposed for non-sinusoidal five-phase PMSMs using only one reduced-order Clarke transformation matrix for each case of faults. New current references are analytically calculated to obtain a constant torque. However, since all d-q current references for control in [15, 16] are time-variant, proportional-integral-resonant controllers with two-resonance frequencies and back-EMF compensation are applied. Another solution to solve the problem of tracking time-variant current references is the use of hysteresis controllers as presented in [17-19]. Phase currents are directly controlled without any transformations. Nevertheless, hysteresis controllers cause variable switching frequencies, more switching losses, high-frequency currents and electromagnetic compatibility problems. Therefore, this solution can be used for low power applications. From the analyses of studies [8-20], a solution to have more constant d-q current references for control in variable-speed drives is interesting, especially at high speed. Recently, [21] has proposed a control structure to use constant current references for post-fault control. However, unequally distributed copper losses and high total copper losses can be observed in [21].

In this paper, a fault-tolerant strategy applying reduced-order transformation matrices is proposed for seven-phase non-sinusoidal PMSMs in a single-phase open-circuit fault. New current references result in similar copper losses in the remaining healthy phases, avoiding overrated currents (overheating) in a particular phase. Especially, the proposed

strategy applies a control structure with time-constant references of main d-q currents (generating most of the torque). It can improve the torque performance with conventional PI controllers at high speed. In this control structure, a real-time current learning process applying a simple adaptive linear neural network (Adaline) is used to extract harmonic components from measured currents in natural frame. Thus, this Adaline-based learning process helps to obtain constant feedback d-q currents for control. Compared to other conventional harmonic extraction methods such as Fast Fourier Transform and Phase-Locked Loop, Adaline gives a better performance because of its online learning, fast convergence, and simple implementation in real time [22].

The paper is organized as follows: Section II describes the modeling of a seven-phase PMSM. Then, new current references with similar copper losses and a new control structure are explained in sections III and IV, respectively. Finally, the proposed strategy is validated by numerical results in section V.

II. Modeling of a Seven-phase PMSM

In this study, a seven-phase PMSM with non-sinusoidal back-EMF is considered. Several hypotheses are described as follows: apart from the 1st harmonic, the back-EMF has a significant proportion of the 3rd harmonic; the machine has seven phases equally shifted and wye-connected; the magnet circuit saturation is not considered in the back-EMF and flux calculations; and iron losses are not considered. The voltage and torque of the machine can be written as follows:

$$\boldsymbol{v} = R_s \boldsymbol{i} + [\boldsymbol{L}]\frac{\mathrm{d}\boldsymbol{i}}{\mathrm{d}t} + \boldsymbol{e} \tag{1}$$

$$T_m = \boldsymbol{e_n}^{\mathrm{T}} \boldsymbol{i} \tag{2}$$

where $\boldsymbol{v}$, $\boldsymbol{i}$, $\boldsymbol{e}$, and $\boldsymbol{e_n}$ are the 7-dimensional vectors of phase voltages, phase currents, back-EMFs and speed-normalized back-EMFs respectively ($\boldsymbol{e_n} = \frac{\boldsymbol{e}}{\Omega}$); Ω is the rotating speed of rotor; R_s is the resistance of stator; $[\boldsymbol{L}]$ is a 7 by 7 stator inductance matrix; T_m is the electromagnetic torque of the machine.

In healthy mode, the conventional rotor field-oriented control (RFOC) is used to control the machine [21]. The classical 7 by 7 Clarke and Park transformation matrices $[\boldsymbol{T_{Clarke}^{classic}}]$ and $[\boldsymbol{T_{Park}^{classic}}]$ are applied to convert the machine parameters from natural frame into d-q frames for control. The current transformation is written as follows:

$$\boldsymbol{i_{dq}}^{\mathrm{T}} = [\boldsymbol{T_{Park}^{classic}}][\boldsymbol{T_{Clarke}^{classic}}]\boldsymbol{i}^{\mathrm{T}} \tag{3}$$

where $\boldsymbol{i} = [i_A\ i_B\ i_C\ i_D\ i_E\ i_F\ i_G]$ and $\boldsymbol{i_{dq}} = [i_{d1}\ i_{q1}\ i_{d2}\ i_{q2}\ i_{d3}\ i_{q3}\ i_y]$.

The seven-phase machine can be mathematically decomposed into 3 fictitious two-phase machines with reference frames (d_1-q_1), (d_2-q_2) and (d_3-q_3) and 1 zero-sequence machine with (y) [23]. A fictitious machine is associated with a given group of harmonics as presented in Table I. The control is simple if each fictitious machine contains only one harmonic, for example the 1st, 9th, 3rd and 7th harmonics. As the wye connection, the zero-sequence current i_y is equal to zero. Therefore, six constant d-q currents (i_{d1}, i_{q1}, i_{d2}, i_{q2}, i_{d3}, i_{q3}) are independently controlled in healthy mode by PI controllers. Current references can be calculated from torque reference with Maximum Torque Per Ampere (MTPA) [17].

TABLE I
Fictitious Machines And Associated Harmonics Of A Seven-phase Machine With Only Odd Harmonics

Fictitious machine	Frame	Associated harmonic ($m \in \mathbb{N}_0$)
1st machine	d_1-q_1	$1, 13 \ldots 7m \pm 1$
2nd machine	d_2-q_2	$5, 9 \ldots 7m \pm 2$
3rd machine	d_3-q_3	$3, 11 \ldots 7m \pm 3$
Zero-sequence machine	y	$7, 21 \ldots 7m$

III. New Current References with Similar Copper Losses

A. New transformation matrices

In fact, the use of new transformation matrices for multiphase non-sinusoidal back-EMF machines in faulty modes has been proposed in studies such as [14, 21]. This approach can be summarized as follows:

1) The use of fundamental current: When phase A is opened, its current is zero. Therefore, the first column of the classical Clarke transformation matrix in [6], associated with phase A, should be removed. The classical Clarke transformation matrix in the post-fault condition $[\boldsymbol{T_{Clarke}^{f}}]$ for a seven-phase machine can be as follows:

$$[\boldsymbol{T_{Clarke}^{f}}] = \sqrt{\frac{2}{7}} \begin{bmatrix} \cos(\delta) & \cos(2\delta) & \cos(3\delta) & \cos(4\delta) & \cos(5\delta) & \cos(6\delta) \\ \sin(\delta) & \sin(2\delta) & \sin(3\delta) & \sin(4\delta) & \sin(5\delta) & \sin(6\delta) \\ \cos(2\delta) & \cos(4\delta) & \cos(6\delta) & \cos(8\delta) & \cos(10\delta) & \cos(12\delta) \\ \sin(2\delta) & \sin(4\delta) & \sin(6\delta) & \sin(8\delta) & \sin(10\delta) & \sin(12\delta) \\ \cos(3\delta) & \cos(6\delta) & \cos(9\delta) & \cos(12\delta) & \cos(15\delta) & \cos(18\delta) \\ \sin(3\delta) & \sin(6\delta) & \sin(9\delta) & \sin(12\delta) & \sin(15\delta) & \sin(18\delta) \\ \sqrt{1/2} & \sqrt{1/2} & \sqrt{1/2} & \sqrt{1/2} & \sqrt{1/2} & \sqrt{1/2} \end{bmatrix} \tag{4}$$

where $\delta = 2\pi/7$ is the spatial displacement angle of two adjacent phases of a seven-phase machine.

In (4), the first, third and fifth row vectors are no longer orthogonal to each other, hence three reference frames (d_1-q_1), (d_2-q_2) and (d_3-q_3) are coupled. Consequently, currents cannot be properly controlled without any reconfigurations.

New transformation matrices for seven-phase non-sinusoidal machines can be determined according to the preservation of the fundamental MMF like in healthy mode. The relationship between new current references in natural frame (i_{B1}, i_{C1}, i_{D1}, i_{E1}, i_{F1}, i_{G1}) and currents in new rotating frames (i_{d11}, i_{q11}, i_{d21}, i_{q21}, i_{x1}, i_{y1}) is described as

$$[i_{B1}\ i_{C1}\ i_{D1}\ i_{E1}\ i_{F1}\ i_{G1}]^{\mathrm{T}} = [\boldsymbol{T_{Clarke}^{1}}]^{-1}[\boldsymbol{T_{Park}^{1}}]^{-1}[i_{d11}\ i_{q11}\ i_{d21}\ i_{q21}\ i_{x1}\ i_{y1}]^{\mathrm{T}} \tag{5}$$

where (i_{d11}, i_{q11}) represent the fundamental space currents; (i_{d21}, i_{q21}) and i_{x1} are the second and third space currents, respectively; i_{y1} is the zero-sequence current (always equal to zero due to the wye connection); index 1 in all variables means that only fundamental currents are considered; $[\boldsymbol{T_{Clarke}^{1}}]$ and $[\boldsymbol{T_{Park}^{1}}]$ are new Clarke and Park 6 by 6 matrices as presented in [21].

New Clarke matrix $[\boldsymbol{T_{Clarke}^{1}}]$ is determined from $[\boldsymbol{T_{Clarke}^{f}}]$ in (4). The remaining row vectors of the new matrix $[\boldsymbol{T_{Clarke}^{1}}]$ are orthogonal to each other, allowing to control independently currents in new rotating frames. If a sinusoidal back-EMF machine is considered, the generated torque is constant. However, the torque has ripples due to interactions between the 1st harmonic of current and the 3rd harmonic of the considered back-EMF. From (2) and (5), the machine torque T_{m1} can be generally described in (6) with an average torque T_{const1} and its harmonics as

$$T_{m1} = T_{const1} + \hat{E}_3 i_{q11}\{f_1(2\theta) + f_2(4\theta)\} + \boldsymbol{e}_{nf}^{\mathrm{T}}\left\{[\boldsymbol{M}_1]\begin{bmatrix} i_{d21} & i_{q21} & i_{x1}\end{bmatrix}^{\mathrm{T}}\right\} \quad (6)$$

$$[\boldsymbol{M}_1] = \begin{bmatrix} 0.363 & 0.521 & 0.232 \\ -0.815 & -0.232 & -0.418 \\ 0.452 & -0.418 & 0.521 \\ 0.452 & 0.418 & -0.521 \\ -0.815 & 0.232 & 0.418 \\ 0.363 & -0.521 & -0.232 \end{bmatrix} \quad (7)$$

where $T_{const1} = \sqrt{7/2}\hat{E}_1 i_{q11}$; $\hat{E}_1$ and $\hat{E}_3$ are the amplitudes of the 1st and 3rd harmonics of $\boldsymbol{e_n}$; θ is the electrical position; f_1 and f_2 are trigonometric functions of 2θ and 4θ respectively; $\boldsymbol{e_{nf}}$ is a 6-dimentional vector of back-EMF derived from $\boldsymbol{e_n}$ by removing the back-EMF of phase A; $[\boldsymbol{M_1}]$ is a constant 6 by 3 matrix in (7) and obtained from the 3rd to 5th columns of $[\boldsymbol{T^1_{Clarke}}]^{-1}$.

In (6), currents (i_{d21}, i_{q21}, i_{x1}) can be used to eliminate the impact of the 1st and 3rd harmonics of $\boldsymbol{e_{nf}}$ on torque ripples by simply imposing currents (i_{d21}, i_{q21}, i_{x1}) to be zero. However, torques with frequencies 2θ and 4θ in T_{m1} cannot be eliminated because of the presence of the 3rd harmonic of back-EMF with amplitude $\hat{E}_3$. Therefore, the 3rd harmonic currents need to be injected to compensate the pulsating torques 2θ and 4θ.

2) The injection of the third harmonic current: The 3rd harmonic currents in natural frame (i_{B3}, i_{C3}, i_{D3}, i_{E3}, i_{F3}, i_{G3}) are calculated from new rotating frame currents (i_{x3}, i_{d23}, i_{q23}, i_{d33}, i_{q33}, i_{y3}) as

$$\begin{bmatrix} i_{B3} & i_{C3} & i_{D3} & i_{E3} & i_{F3} & i_{G3}\end{bmatrix}^{\mathrm{T}} = [\boldsymbol{T^3_{Clarke}}]^{-1}[\boldsymbol{T^3_{Park}}]^{-1}\begin{bmatrix} i_{x3} & i_{d23} & i_{q23} & i_{d33} & i_{q33} & i_{y3}\end{bmatrix}^{\mathrm{T}} \quad (8)$$

where (i_{d33}, i_{q33}) represent the 3rd harmonic space currents while i_{x3} and (i_{d23}, i_{q23}) are the first and second space currents; i_{y3} is the zero-sequence current (always equal to zero due to the wye connection); index 3 in all variables means that third harmonic currents are considered; $[\boldsymbol{T^3_{Clarke}}]$ and $[\boldsymbol{T^3_{Park}}]$ are new Clarke and Park 6 by 6 matrices as presented in [21].

$[\boldsymbol{T^3_{Clarke}}]$ is defined from matrix $[\boldsymbol{T^{fault}_{Clarke}}]$ in (4) to obtain the orthogonality property of its row vectors, enabling to control independently currents in the new rotating frames. From (2) and (5) and (8), the total torque T_{m13} can be expressed as

$$T_{m13} = T_{const13} + \left\{\hat{E}_3 i_{q11} + \hat{E}_1 i_{q33}\right\}\{f_1(2\theta) + f_2(4\theta)\} + \boldsymbol{e}_{nf}^{\mathrm{T}}\left\{[\boldsymbol{M}_1]\begin{bmatrix} i_{d21} & i_{q21} & i_{x1}\end{bmatrix}^{\mathrm{T}} + [\boldsymbol{M}_3]\begin{bmatrix} i_{x3} & i_{d23} & i_{q23}\end{bmatrix}^{\mathrm{T}}\right\} \quad (9)$$

$$[\boldsymbol{M}_3] = \begin{bmatrix} 0.418 & -0.452 & 0.521 \\ 0.521 & -0.363 & -0.232 \\ 0.232 & 0.815 & -0.418 \\ -0.232 & 0.815 & 0.418 \\ -0.521 & -0.363 & 0.232 \\ -0.418 & -0.452 & -0.521 \end{bmatrix} \quad (10)$$

where $T_{const13} = \sqrt{7/2}\left(\hat{E}_1 i_{q11} + \hat{E}_3 i_{q33}\right)$; $[\boldsymbol{M_3}]$ is a constant 6 by 3 matrix in (10) obtained from the 1st to 3rd columns of $[\boldsymbol{T^3_{Clarke}}]^{-1}$.

From (9), to eliminate torque ripples 2θ and 4θ, the 3rd harmonic space current i_{q33} needs to be calculated as

$$i_{q33} = -(\hat{E}_3 / \hat{E}_1) i_{q11}\,. \quad (11)$$

B. Proposed Similar Copper Losses (SCL)

To eliminate the impacts of harmonics of $\boldsymbol{e_{nf}}$ in (9), currents (i_{d21}, i_{q21}, i_{x1}) and (i_{x3}, i_{d23}, i_{q23}) can be defined according to two current design options: Robust Control Approach (RCA) and Similar Copper Losses (SCL). Indeed, RCA has been presented in [21]. The six currents (i_{d21}, i_{q21}, i_{x1}) and (i_{x3}, i_{d23}, i_{q23}) are imposed to be zero. Therefore, besides the 1st and 3rd harmonics,

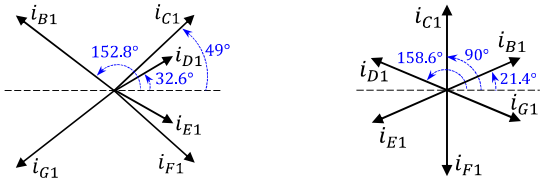

Fig. 1. The 1st harmonics of the 6 healthy phase currents designed by RCA (a), and by SCL (b) with an open-circuit fault in phase A.

if the back-EMF contains other harmonics such as the 9th harmonic in the second fictitious machine (Table I), the generated torque T_{m13} is still constant and equal to $T_{const13}$ according to (9). Thus, RCA has robustness. The 1st harmonic components of the six healthy phase currents in natural frame are shown in Fig. 1a. Notably, their amplitudes are very different, probably causing overheating in phases B and G.

In this study, the current design option SCL is proposed. Its main idea is to distribute similarly copper losses to all remaining healthy phases, hence, the local thermal limit of each phase winding can be respected. Due to the back-EMF harmonic property, the 3rd harmonic currents account for a small proportion compared to the 1st harmonic currents. Therefore, RMS currents as well as copper losses mainly depend on the 1st harmonic currents. Then, the 1st harmonic components of the 6 healthy phase currents in natural frame can be designed according to [3] as follows:

$$i_{B1} = 0.6591 i_{q11}\sin(\theta + 21.4^0) \quad (12)$$

$$i_{C1} = 0.6591 i_{q11}\sin(\theta + 90^0) \quad (13)$$

$$i_{D1} = 0.6591 i_{q11}\sin(\theta + 158.6^0) \quad (14)$$

$$i_{E1} = 0.6591 i_{q11}\sin(\theta - 158.6^0) \quad (15)$$

$$i_{F1} = 0.6591 i_{q11}\sin(\theta - 90^0) \quad (16)$$

$$i_{G1} = 0.6591 i_{q11}\sin(\theta - 21.4^0) \quad (17)$$

It is noted that their amplitudes are designed to be identical as shown in (12)-(17) and Fig. 1b. Whereas currents (i_{d11}, i_{q11}, i_{d33}, i_{q33}), generating torque, are constant, currents (i_{d21}, i_{q21}, i_{x1}) need to be calculated from (5), (12)-(17) as follows:

$$i_{d21} = -\frac{\sin(6\pi/7)}{\sin(5\pi/7)}\left(i_{d11}\cos(\theta) - i_{q11}\sin(\theta)\right) \quad (18)$$

$$i_{q21} = \sqrt{8/7}\sin(6\pi/7)\left[\left(\frac{i_{d11}\sin(\theta) + i_{q11}\cos(\theta)}{\sqrt{8/7}\sin(3\pi/7)} - i_{C1}\right)\left(\frac{\cos(3\pi/7)}{\cos(2\pi/7)}\right) - i_{C1}\right] \quad (19)$$

$$i_{x1} = \sqrt{8/7}\sin(2\pi/7)\left[\left(\frac{i_{d11}\sin(\theta) + i_{q11}\cos(\theta)}{\sqrt{8/7}\sin(3\pi/7)} - i_{C1}\right)\left(\frac{\cos(\pi/7)}{\cos(2\pi/7)}\right) - i_{C1}\right]. \quad (20)$$

However, from (9), as currents (i_{d21}, i_{q21}, i_{x1}) are time-variant, these currents interact with harmonics of back-EMF (1st, 3rd,…) in $\boldsymbol{e_{nf}}$, causing torque ripples. Thus, from (8)-(9), currents (i_{d23}, i_{q23}, i_{x3}) eliminating the torque ripples caused by the 1st and 3rd harmonics of back-EMF are written as

$$i_{d23} = -\frac{\sin(6\pi/7)}{\sin(5\pi/7)}\left(i_{d33}\cos(3\theta) - i_{q33}\sin(3\theta)\right) \quad (21)$$

$$i_{q23} = \sqrt{8/7}\sin(6\pi/7)\left[\left(\frac{i_{d33}\sin(3\theta) + i_{q33}\cos(3\theta)}{\sqrt{8/7}\sin(3\pi/7)} - i_{C3}\right)\left(\frac{\cos(3\pi/7)}{\cos(2\pi/7)}\right) - i_{C3}\right] \quad (22)$$

$$i_{x3} = \sqrt{8/7}\sin(2\pi/7)\left[\left(\frac{i_{d33}\sin(3\theta) + i_{q33}\cos(3\theta)}{\sqrt{8/7}\sin(3\pi/7)} - i_{C3}\right)\left(\frac{\cos(\pi/7)}{\cos(2\pi/7)}\right) - i_{C3}\right] \quad (23)$$

$$i_{C3} = 0.659 I_{q33} \sin(3\theta + 90^0) \quad (24)$$

where i_{C3} is the 3rd harmonic component of phase-C current in (24).

From (9), (11)-(24), the total torque T_{m13} can be expressed as

$$T_{m13} = T_{const13} = \sqrt{7/2}\left(\hat{E}_1 i_{q11} + \hat{E}_3 i_{q33}\right). \quad (25)$$

It is noted that T_{m13} in (25) is constant when the 1st and 3rd harmonics of back-EMF are considered. If the back-EMF has other harmonics (9th, for example), torque ripples may appear due to the interaction between these back-EMF harmonics and 6 variable currents (i_{d21}, i_{q21}, i_{x1}) and (i_{x3}, i_{d23}, i_{q23}). Notably, a lower total copper loss and evenly distributed copper losses in phases are the advantages of SCL.

IV. Current Control Structure Applying Adaline

The current control structure using constant d-q current references with RCA for post-fault control has been proposed in [21]. Fig. 2a describes the control structure when phase A is opened. Reference values of currents (i_{d11}, i_{q11}, i_{d21}, i_{q21}, i_{x1}, i_{y1}) and (i_{x3}, i_{d23}, i_{q23}, i_{d33}, i_{q33}, i_{y3}) are directly used for control. This structure facilitates the current control using simple controllers such as PI with constant d-q current references. Because zero-sequence currents (i_{y1}, i_{y3}) are always equal to zero due to the wye-connected stator windings, their controllers are not necessary. Thus, ten PI controllers are used to control 10 d-q currents in which at least 4 currents (i_{d11}, i_{q11}, i_{d33}, i_{q33}) mainly generating torque are constant, allowing to improve torque quality. Six d-q currents (i_{d21}, i_{q21}, i_{x1}, i_{x3}, i_{d23}, i_{q23}) that do not contribute to the average torque can be constant or time-variant based on current design options RCA and SCL. The output signals of PI controllers, voltage references in d-q frames, are converted into natural frame by using inversions of new transformation matrices ($[\boldsymbol{T}^{\mathbf{1}}_{\boldsymbol{Clarke}}]^{-1}$, $[\boldsymbol{T}^{\mathbf{1}}_{\boldsymbol{Park}}]^{-1}$, $[\boldsymbol{T}^{\mathbf{3}}_{\boldsymbol{Clarke}}]^{-1}$, $[\boldsymbol{T}^{\mathbf{3}}_{\boldsymbol{Park}}]^{-1}$). Then, the sums of the voltage harmonics of each phase in natural frame are used to calculate the duty cycle and Pulse Width Modulation (PWM) signals for the seven-phase inverter.

The measured currents of the healthy phases are provided to extract useful harmonics of measured phase currents by the real-time current learning process (RTCL). From the back-EMF assumption, the 1st and 3rd harmonics are considered as useful harmonics in this study. RTCL facilitates the use of new transformation matrices ($[\boldsymbol{T}^{\mathbf{1}}_{\boldsymbol{Clarke}}]^{-1}$, $[\boldsymbol{T}^{\mathbf{1}}_{\boldsymbol{Park}}]^{-1}$, $[\boldsymbol{T}^{\mathbf{3}}_{\boldsymbol{Clarke}}]^{-1}$, $[\boldsymbol{T}^{\mathbf{3}}_{\boldsymbol{Park}}]^{-1}$) to obtain estimated constant d-q currents for feedback (response) signals of PI controllers. If these harmonics are not separated, constant feedback currents cannot be obtained because one transformation matrix for the two harmonics (1st and 3rd) do not exist [13, 14, 21].

The most important part of RTCL is an Adaline that is presented in Fig. 2b. It separates harmonics of the measured current of only one arbitrary phase in the remaining healthy phases (phase B, for example). Then, the other phase currents are derived from the Adaline-based estimated current (phase B) according to their mathematical relationships in current design options (RCA or SCL). Notably, SCL with (12)-(17) is the contribution of this present study. The Adaline structure includes four inputs (1st and 3rd harmonics), four weights (constant values), and one output (estimated current). Its learning process (weight updating) depends on the updating rule (Least Mean Square - LMS) and the learning rate η. A proper value of η can guarantee stability of the system ($0<\eta<1$). More details about the Adaline design can be found in [21].

V. Numerical Verification

A. Studied multiphase drive description

To verify the proposed strategy SCL, a seven-phase electric drive is studied. Parameters of the machine drive are described in Table II. A 7-leg voltage source inverter with a PWM frequency of 10 kHz fed by DC-bus voltage supplies the seven-phase PMSM. The speed-normalized non-sinusoidal back-EMF waveform is shown in Fig. 3. The 3rd harmonic amplitude is equal to 32.3% of the 1st harmonic amplitude.

To validate the strategy, the torque ripple, denoted by ΔT, can be expressed as

$$\Delta T = \frac{T_{max} - T_{min}}{T_{average}} 100\% \quad (26)$$

where T_{max}, T_{min}, and $T_{average}$ are maximum, minimum, and average values of the machine torque T_{m13}, respectively.

B. Calculated results

Calculated results are obtained from reference values without PI current controllers, PWM, and an inverter. To respect the rated RMS current of 5.1 A, the current references $i_{q11} = 7.5$ A and $i_{q33} = -2.4$ A must be imposed in faulty mode, leading to a torque of 15.9 N.m. Both RCA and SCL theoretically generate constant torques with the considered back-EMF.

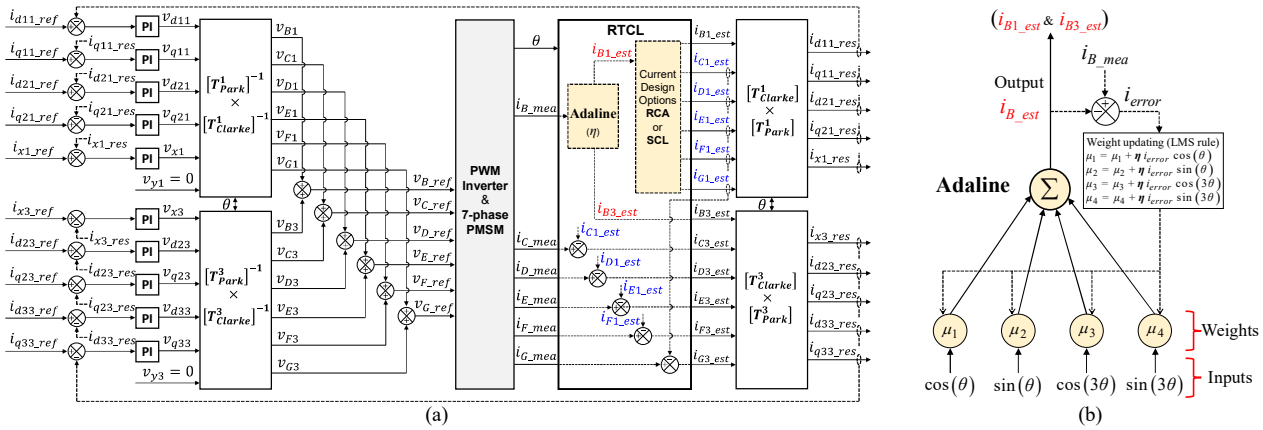

Fig. 2. The new current control structure with more constant d-q current references when phase A is open-circuited.

TABLE II
ELECTRICAL PARAMETERS OF THE STUDIED SEVEN-PHASE MACHINE DRIVE

Parameter	Value
Stator resistance R_s (Ω)	1.4
Self-inductance L (mH)	14.7
Mutual inductance M_1 (mH)	3.5
Mutual inductance M_2 (mH)	-0.9
Mutual inductance M_3 (mH)	-6.1
1st harmonic of speed-normalized back-EMF (V/rad/s)	1.3
3rd harmonic of back-EMF over 1st harmonic (%)	32.3
Number of pole pairs p	3
Rated rotating speed (rpm)	750
Rated RMS current of seven-phase PMSM (A)	5.1

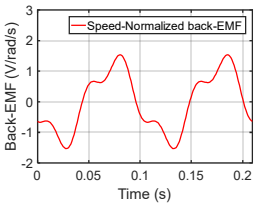

Fig. 3. Speed-normalized back-EMF of the studied seven-phase machine.

In healthy mode, MTPA [17] is used to calculated current references to generate the same torque (15.9 Nm), facilitating comparisons in terms of currents and copper losses. Phase current references in healthy mode at 750 rpm (the rated speed) are shown in Fig. 4a. In faulty mode, total current references for the remaining healthy phases with RCA and SCL at 750 rpm are shown in Figs. 4b and 4c, respectively. The maximum peak current with SCL (6.8 A) is 31% lower than that of RCA (8.9 A). The calculated per phase and total copper losses compared to healthy mode are described in Table III. Per unit (pu) is used to describe the changes of copper losses in faulty mode compared to healthy mode. It is noted that calculated copper losses with SCL in the remaining healthy phases are similar. These values are between 2.25 and 2.42 pu (an increase of 7.6%). Meanwhile, those by RCA vary from 0.7 to 2.9 times (an increase of 300%). Especially, SCL generates a total copper loss (1.98 pu) that is 16% lower than RCA does (2.3 pu).

C. Simulated results

Simulated results are obtained from the model of the studied drive in MATLAB/Simulink with PI current controllers, and a voltage source inverter controlled by PWM. To make comparisons, an operation includes three stages as follows:

1) Stage 1: The studied drive operates in healthy mode with RFOC scheme and MTPA strategy.
2) Stage 2: An open-circuit fault of phase A happens without any reconfigurations.
3) Stage 3: New current references with RCA or SCL are imposed in the new control scheme using Adaline with the learning rate η=0.0001.

From Fig. 5, the simulated torque ripple is lowest at 6.3% in healthy mode. When phase A is opened, the torque ripple increases to 35%. The new scheme with RCA or SCL can significantly reduce the torque ripple. SCL has a slightly higher simulated torque ripple (12%) than RCA does (9.5%) because SCL requires the control of six time-variant currents (i_{d21}, i_{q21}, i_{x1}, i_{x3}, i_{d23}, i_{q23}). Current responses of (i_{d21}, i_{q21}, i_{x1}) obtained from the learning process of Adaline are almost the same as their references. The control performance of (i_{x3}, i_{d23}, i_{q23}) is presented in Fig. 6. Phase currents (response signals) with RCA and SCL are shown in Fig. 7. The simulated results are in good

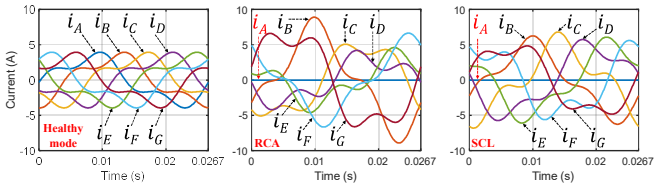

(a) (b) (c)

Fig. 4. (Calculated result) Phase current references in healthy mode (a), total current references for the remaining healthy phases when phase A is opened with RCA (b), and by proposed SCL (c), at 750 rpm.

TABLE III
COPPER LOSSES IN POST-FAULT OPERATION WITH RCA AND SCL COMPARED TO HEALTHY MODE FOR THE SAME TORQUE AT 750 RPM

Phase	RCA [21]		Proposed SCL	
	Calculated (pu)	Simulated (pu)	Calculated (pu)	Simulated (pu)
B	4.45	4.61	2.25	2.37
C	2.52	2.54	2.42	2.44
D	1.11	1.12	2.27	2.32
E	1.11	1.12	2.27	2.31
F	2.52	2.55	2.42	2.46
G	4.45	4.51	2.25	2.33
Total	2.3	2.33	1.98	2.01

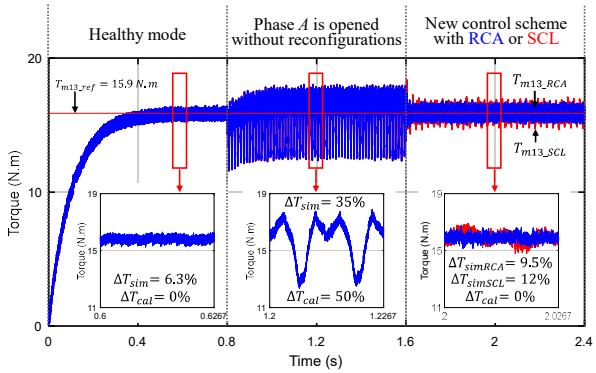

Fig. 5. (Simulated result) Torque in the 3-stage operation with new current references by RCA and proposed SCL in the new control scheme at 750 rpm.

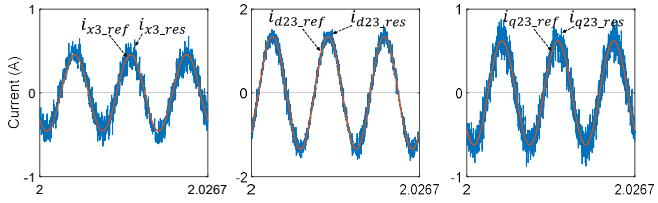

(a) (b) (c)

Fig. 6. (Simulated result) Control performance of currents i_{x3} (a), i_{d23} (b), and i_{q23} (c), with proposed SCL in the new control scheme when phase A is opened at 750 rpm.

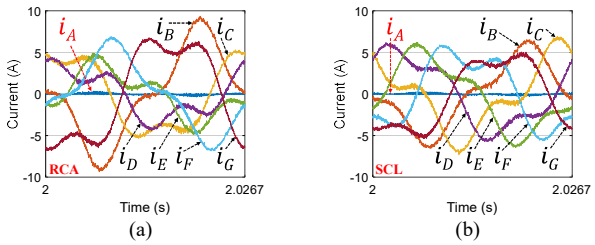

(a) (b)

Fig. 7. (Simulated result) Phase currents with RCA and proposed SCL in the new control scheme at 750 rpm when phase A is opened.

accordance with the calculated (reference) results in Fig. 4. The simulated copper losses are summarized in Table III. Although SCL has a slightly higher simulated torque ripple compared to RCA, it generates a lower total copper loss (2.01 pu with SCL compared to 2.33 pu with RCA) and evenly distributed copper

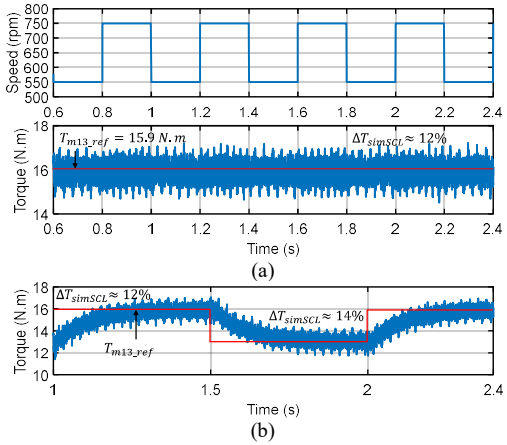

Fig. 8. (Simulated result) Torque performance under the variation of the rotating speed (a) and the variation of torque reference (b), using proposed SCL in the new control scheme.

losses in the remaining healthy phases (2.31 to 2.46 pu for SCL, 1.12 to 4.61 pu for RCA).

The dynamic performance of the new control structure using SCL is shown in Fig. 8 under variations of the rotating speed and torque reference. It is noted that the speed variation from 550 rpm to 750 rpm does not have impact on torque generation ($\Delta T \approx 12\%$). The variation of torque reference from 12.9 N.m to 15.9 N.m makes the torque ripple vary from about 12% to 14% due to the variation of the average torque. The transient time is about 0.3 s with a Adaline learning rate of η=0.0001.

VI. Conclusion

The paper has proposed a fault-tolerant strategy in which classical PI controllers for main currents (generating torque) are facilitated with constant references under faulty mode. Especially, with new current references, copper losses are well distributed in the remaining healthy phases. It can avoid exceeding local thermal limits of stator windings. In addition, total copper losses have been reduced compared to the existing study. A seven-phase non-sinusoidal machine has been chosen for validation but the machine with other phase numbers can be applied. When another phase or more phases are open-circuited, the proposed control strategy can be adapted with new transformation matrices.

Acknowledgement

We would like to thank the CE2I project sponsored by European Regional Development Fund, French State, and French Region of Hauts-de-France for the financial support.

References

[1] E. Levi, "Multiphase Electric Machines for Variable-Speed Applications," *IEEE Transactions on Industrial Electronics,* vol. 55, no. 5, pp. 1893-1909, 2008.

[2] M. J. Duran and F. Barrero, "Recent Advances in the Design, Modeling, and Control of Multiphase Machines Part II," *IEEE Transactions on Industrial Electronics,* vol. 63, no. 1, pp. 459-468, 2016.

[3] F. Jen-Ren and T. A. Lipo, "Disturbance-free operation of a multiphase current-regulated motor drive with an opened phase," *IEEE Transactions on Industry Applications,* vol. 30, no. 5, pp. 1267-1274, 1994.

[4] H. A. Toliyat, "Analysis and simulation of five-phase variable-speed induction motor drives under asymmetrical connections," *IEEE Transactions on Power Electronics,* vol. 13, no. 4, pp. 748-756, 1998.

[5] Y. Sui, P. Zheng, Z. Yin, M. Wang, and C. Wang, "Open-Circuit Fault-Tolerant Control of Five-Phase PM Machine Based on Reconfiguring Maximum Round Magnetomotive Force," *IEEE Transactions on Industrial Electronics,* vol. 66, no. 1, pp. 48-59, 2019.

[6] F. Locment, E. Semail, and X. Kestelyn, "Vectorial Approach-Based Control of a Seven-Phase Axial Flux Machine Designed for Fault Operation," *IEEE Transactions on Industrial Electronics,* vol. 55, no. 10, pp. 3682-3691, 2008.

[7] D. T. Vu, N. K. Nguyen, E. Semail, and T. J. d. S. Moraes, "Control strategies for non-sinusoidal multiphase PMSM drives in faulty modes under constraints on copper losses and peak phase voltage," *IET Electric Power Applications*, vol. 13, no. 11, pp. 1743-1752, 2019.

[8] R. Hyung-Min, K. Ji-Woong, and S. Seung-Ki, "Synchronous-frame current control of multiphase synchronous motor under asymmetric fault condition due to open phases," *IEEE Transactions on Industry Applications,* vol. 42, no. 4, pp. 1062-1070, 2006.

[9] H. Guzmán, M. J. Durán, and F. Barrero, "A comprehensive fault analysis of a five-phase induction motor drive with an open phase," in *15th International Power Electronics and Motion Control Conference (EPE/PEMC)*, Novi Sad, Serbia, 2012, pp. LS5b.3-1-LS5b.3-6.

[10] H. Guzman *et al.*, "Comparative Study of Predictive and Resonant Controllers in Fault-Tolerant Five-Phase Induction Motor Drives," *IEEE Transactions on Industrial Electronics,* vol. 63, no. 1, pp. 606-617, 2016.

[11] B. Tian, Q. T. An, J. D. Duan, D. Y. Sun, L. Sun, and D. Semenov, "Decoupled Modeling and Nonlinear Speed Control for Five-Phase PM Motor Under Single-Phase Open Fault," *IEEE Transactions on Power Electronics,* vol. 32, no. 7, pp. 5473-5486, 2017.

[12] H. Zhou, W. Zhao, G. Liu, R. Cheng, and Y. Xie, "Remedial Field-Oriented Control of Five-Phase Fault-Tolerant Permanent-Magnet Motor by Using Reduced-Order Transformation Matrices," *IEEE Transactions on Industrial Electronics,* vol. 64, no. 1, pp. 169-178, 2017.

[13] D. T. Vu, N. K. Nguyen, and E. Semail, "An Overview of Methods using Reduced-Ordered Transformation Matrices for Fault-Tolerant Control of 5-phase Machines with an Open Phase," in *2019 IEEE International Conference on Industrial Technology (ICIT)*, Melbourne, Australia, 2019, pp. 1557-1562.

[14] G. Liu, Z. Lin, W. Zhao, Q. Chen, and G. Xu, "Third Harmonic Current Injection in Fault-Tolerant Five-Phase Permanent-Magnet Motor Drive," *IEEE Transactions on Power Electronics,* vol. 33, no. 8, pp. 6970 - 6979, 2018.

[15] C. Xiong, H. Xu, T. Guan, and P. Zhou, "Fault-tolerant FOC for five-phase SPMSM with non-sinusoidal back EMF," *IET Electric Power Applications*, vol. 13, no. 11, pp. 1734-1742, 2019.

[16] C. Xiong, T. Guan, P. Zhou, and H. Xu, "A Fault-Tolerant FOC Strategy for Five-Phase SPMSM With Minimum Torque Ripples in the Full Torque Operation Range Under Double-Phase Open-Circuit Fault," *IEEE Transactions on Industrial Electronics,* vol. 67, no. 11, pp. 9059-9072, 2020.

[17] X. Kestelyn and E. Semail, "A Vectorial Approach for Generation of Optimal Current References for Multiphase Permanent-Magnet Synchronous Machines in Real Time," *IEEE Transactions on Industrial Electronics,* vol. 58, no. 11, pp. 5057-5065, 2011.

[18] A. Mohammadpour and L. Parsa, "Global Fault-Tolerant Control Technique for Multiphase Permanent-Magnet Machines," *IEEE Transactions on Industry Applications,* vol. 51, no. 1, pp. 178-186, 2015.

[19] M. Bermudez, I. Gonzalez-Prieto, F. Barrero, H. Guzman, M. J. Duran, and X. Kestelyn, "Open-Phase Fault-Tolerant Direct Torque Control Technique for Five-Phase Induction Motor Drives," *IEEE Transactions on Industrial Electronics,* vol. 64, no. 2, pp. 902-911, 2017.

[20] F. Lin, Y. Hung, and M. Tsai, "Fault-Tolerant Control for Six-Phase PMSM Drive System via Intelligent Complementary Sliding-Mode Control Using TSKFNN-AMF," *IEEE Transactions on Industrial Electronics,* vol. 60, no. 12, pp. 5747-5762, 2013.

[21] D. T. Vu, N. K. Nguyen, and E. Semail, "Fault-Tolerant Control for Nonsinusoidal Multiphase Drives With Minimum Torque Ripple," *IEEE Transactions on Power Electronics,* vol. 37, no. 6, pp. 6290-6304, 2022.

[22] N. K. Nguyen, D. Flieller, P. Wira, and D. O. Abdeslam, "Neural networks for phase and symmetrical components estimation in power systems," in *2009 35th Annual Conference of IEEE Industrial Electronics*, Porto, Portugal, 2009, pp. 3252-3257.

[23] E. Semail, X. Kestelyn, and A. Bouscayrol, "Right harmonic spectrum for the back-electromotive force of an n-phase synchronous motor," in *the 39th IEEE Industry Applications Conference*, Seattle, WA, USA, 10/2004, vol. 1, pp. 71-78.